

## Magnetic Excitations in Cu<sub>6</sub> and Mn<sub>6</sub> Hexagons Embedded in D<sub>3d</sub>-Symmetric Polyoxotungstates

Noa Zamstein, Alex Tarantul, and Boris Tsukerblat\*

Department of Chemistry, Ben-Gurion University of the Negev, 84105 Beer-Sheva, Israel

Received March 28, 2007

In this article we reconsider the discussion of the magnetic measurements for the two novel polyoxotungstates,  $(n\text{-BuNH}_3)_{12}[(\text{CuCl})_6(\text{AsW}_9\text{O}_{33})_2]\cdot 6\text{H}_2\text{O}$  and  $(n\text{-BuNH}_3)_{12}[(\text{MnCl})_6(\text{SbW}_9\text{O}_{33})_2]\cdot 6\text{H}_2\text{O}$ , which have been synthesized and characterized by Yamase et al. (*Inorg.Chem.* **2006**, *45*, 7698). Analysis of the magnetic susceptibility and magnetization for Cu<sub>6</sub><sup>12+</sup> and Mn<sub>6</sub><sup>12+</sup> hexagons based on the exact diagonalization of isotropic exchange Hamiltonian shows that the best-fit first-neighbor coupling parameters are  $J = 35$  and  $0.55\text{ cm}^{-1}$ , respectively, while the second-neighbor interactions are very small. These values exceed considerably those obtained by Yamase et al. ( $J = 8.82$  and  $0.14\text{ cm}^{-1}$ ) on the basis of the Kambe–Van Vleck formula that is inappropriate for six-membered rings. We also got perfect fits to the experimental data for the field dependence of magnetization at 1.8 K. The results imply the importance of axial anisotropy, which is shown to be especially pronounced for the Mn<sub>6</sub><sup>12+</sup> cluster. We discuss also the symmetry assignments of exchange multiplets to the exact  $S\Gamma$  terms (full spin,  $S$ , and irreducible representation,  $\Gamma$ , of the point group) and correlate the results with the selection rules for the anisotropic magnetic contributions. The antisymmetric exchange is shown to appear in orbitally degenerate multiplets as a first-order perturbation and gives rise to an easy axis of magnetization along the C<sub>6</sub> axis. Evaluation of the Zeeman levels shows that the field applied in the plane of the hexagon fully reduces the effect of the antisymmetric exchange.

### 1. Introduction

Polyoxometalates (POMs) form a large and distinctive class of inorganic compounds, which have been the focus of interest of many branches of science in recent years, such as chemistry, biology, medicine, and materials science.<sup>1</sup> This is the result of the high versatility of their electronic and structural variation, which has rendered these compounds model systems for studying metal–oxide-based conductivity, intramolecular and intermolecular electron transfer in mixed-

valence systems, magnetic interactions, and electron–spin couplings in large clusters. In particular, there has been extensive research aimed toward designing single-molecule magnets based on POMs encapsulating metal clusters (see recent book by Gatteschi et al.<sup>2</sup> highlighting this area). Polyoxotungstates are one of the most important classes of POMs in this context. This is because of their lability and reactivity, enabling them to act as ligands toward 3d-transition metal ions, creating clusters of varying sizes and topologies. The bulky nonmagnetic POM framework guarantees an effective magnetic isolation of the metal clusters, while also imposing its geometry, thus providing good opportunities for the study of exchange interactions and electron delocalization.<sup>3,4</sup>

In this paper, we discuss the magnetic data on two novel polyoxotungstates,  $(n\text{-BuNH}_3)_{12}[(\text{CuCl})_6(\text{AsW}_9\text{O}_{33})_2]\cdot 6\text{H}_2\text{O}$  and  $(n\text{-BuNH}_3)_{12}[(\text{MnCl})_6(\text{SbW}_9\text{O}_{33})_2]\cdot 6\text{H}_2\text{O}$ , which have

\* To whom correspondence should be addressed. E-mail address: tsuker@bgu.ac.il.

(1) (a) Pope, M. T.; Müller, A., Eds. *Polyoxometalates: From Platonic Solids to Anti-Retroviral Activity*; Kluwer: Dordrecht, The Netherlands, 1994. (b) Hill, C., Ed. *Polyoxometalates*. In *Chemical Reviews*; American Chemical Society: Washington, DC, 1998. (c) Pope, M. T.; Müller, A., Eds. *Polyoxometalate Chemistry: From Topology via Self-Assembly to Applications*; Kluwer: Dordrecht, The Netherlands, 2001. (d) Yamase, T.; Pope, M. T., Eds. *Polyoxometalate Chemistry for Nano-Composite Design*; Kluwer: Dordrecht, The Netherlands, 2002. (e) Borrás-Almenar, J. J.; Coronado, E.; Müller, A.; Pope, M. T., Eds. *Polyoxometalate Molecular Science*; NATO Science Series; Kluwer: Dordrecht, The Netherlands, 2003; Vol. 98. (f) Kortz, U.; Hussain, F.; Reicke, M. *Angew. Chem., Int. Ed.* **2005**, *44*, 3773–3777. (g) Nellutla, S.; van Tol, J.; Dalal, N. S.; Bi, L.-H.; Kortz, U.; Keita, B.; Nadjro, L.; Khitrov, G. A.; Marshall, A. G. *Inorg. Chem.* **2005**, *44*, 9795–9806.

(2) Gatteschi, D.; Sessoli, R.; Villian, J. *Molecular Nanomagnets*; Oxford University Press: Oxford, U.K., 2006.

(3) (a) Clemente-Juan, J. M.; Coronado, E. *Coord. Chem. Rev.* **1999**, *361*, 193–195, 361–394. (b) Clemente-Juan, J. M.; Coronado, E.; Forment-Aliaga, A.; Galan-Mascaros, J. R.; Gimenez-Saiz, C.; Gomez-Garcia, C. *Inorg. Chem.* **2004**, *43*, 2689–2694.

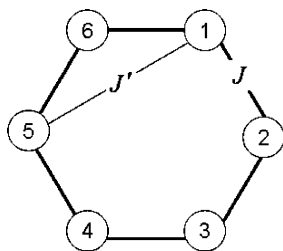


**Figure 1.** Scheme of the first- and second-neighbor exchange interactions in a hexagon.

recently been synthesized and characterized by Yamase et al.<sup>5</sup> These complexes are  $D_{3d}$ -symmetric, and six 5-fold coordinated metal ions form approximately equatorial hexagons ( $\text{Cu}_6^{12+}$  and  $\text{Mn}_6^{12+}$  clusters, hereafter  $\text{Cu}_6$  and  $\text{Mn}_6$ ) with the first-neighbor  $\text{Cu}\cdots\text{Cu}$  and  $\text{Mn}\cdots\text{Mn}$  distances of 2.913 and 3.248 Å, respectively.<sup>5</sup> Yamase et al.<sup>5</sup> also reported the magnetic behavior of these compounds and provided clear evidence of the ferromagnetic character of the exchange interaction, but the modeling of the magnetic properties was based on the Kambe–Van Vleck formula (see text) that is irrelevant to the case of spin ring and leads to an improper estimation of the exchange parameters.

We attempt to reconsider the interpretation of the experimental magnetic data<sup>5</sup> for the two POMs mentioned above on the basis of the full energy pattern obtained with the aid of the irreducible tensor operators (ITO) technique<sup>6</sup> and Magpack software.<sup>7</sup> We discuss also the relationship between the features of the exact energy pattern and that based on the model employed in ref 5.

The outline of the paper is as follows. In section 2, we describe the energy pattern for the  $\text{Cu}_6$  and  $\text{Mn}_6$  clusters; section 3 is devoted to the discussion of the symmetry properties of the exchange multiplets. The group theoretical assignment of the exchange multiplets to the exact  $S\Gamma$  terms of the system (full spin  $S$  and irreducible representation  $\Gamma$  of the point group) shows the presence of orbitally degenerate states that exhibit first-order splitting caused by the anti-symmetric (AS) exchange. The problem of degeneracy in the energy pattern of spin rings is also discussed in view of the magnetic anisotropy. Section 4 gives the results of our calculations of the magnetic susceptibility and magnetization versus field, as well as the processing of the experimental data of Yamase et al.<sup>5</sup> We propose a new set of exchange parameters for these systems and find the parameters of the axial anisotropy for the ferromagnetic ground states.

## 2. Energy Pattern

Because the metal ions in the compound under consideration occupy low-symmetry sites, the orbital degeneracy of the ground terms of the constituent ions is completely removed, and one can model the isotropic superexchange interaction by the conventional Heisenberg–Dirac–Van Vleck (HDVV) Hamiltonian<sup>2</sup>

$$H = -2J(S_1S_2 + S_2S_3 + S_3S_4 + S_4S_5 + S_5S_6 + S_6S_1) - 2J'(S_1S_3 + S_2S_4 + S_3S_5 + S_5S_1 + S_2S_6 + S_6S_4) \equiv H_0 + H' \quad (1)$$

In eq 1, the parameters  $J$  and  $J'$  refer to the first- and second-neighbor exchange interactions (Hamiltonians  $H_0$  and  $H'$ ) in accordance with the enumeration of the sites in the hexagons with magnetically equivalent sites as shown in Figure 1, and  $S_i$  represents the total spins of the ions ( $S_i = 1/2$  for  $\text{Cu}^{2+}$  ions and  $S_i = 5/2$  for  $\text{Mn}^{2+}$ ). Third-order and higher interactions are assumed to be negligible.

The energy levels of the spin hexagons within the first-neighbor coupling approximation (eigen-values of  $H_0$ ) have been modeled in ref 5 by the well-known Kambe's formula applied to the six exchange-coupled ions

$$E(S) = -J[S(S+1) - 6S_i(S_i+1)] \quad (2)$$

where  $S$  is the full spin of the system ( $0 \leq S \leq 3$  for  $\text{Cu}_6$  and  $0 \leq S \leq 15$  for  $\text{Mn}_6$ ). In fact, the Kambe's formula, eq 6, provides the exact solution to the exchange problem only in some special cases of high symmetry when the exchange Hamiltonian can be expressed through the operator  $S^2 = (\sum_i S_i)^2$  and thus can be represented as

$$H = -2J \sum_{ij} S_i S_j \quad (3)$$

An equation of type 2 has been proposed by Van Vleck<sup>8</sup> which served as an approximation in his consideration of ferromagnetism in solids. An exact solution to the exchange problem for a restricted number of symmetric clusters has been obtained by Kambe (for a review see refs 2 and 6) when the energy levels depend on of full and intermediate spin quantum numbers. Later, the Van Vleck approximation was applied to finite chains,<sup>9</sup> assuming that each ion is coupled to a certain mean number of neighbors, and consequently, the energy levels are expressed by Kambe's formula.<sup>5</sup> The resulting Kambe's expression is usually referred to as the Van Vleck formula (ref 5). The most systematic study of the soluble (Kambe's) systems has been presented by Belorizky and Fries.<sup>10</sup>

The Hamiltonian, eq 3 is strictly valid for clusters in which each spin is equally coupled to all remaining ones (this will be referred to as "spherical" model) that occurs only in three topologies, namely, for the trivial case of a dimer, an equilateral triangle and a regular tetrahedron. In these special

(4) (a) Borrás-Almenar, J. J.; Clemente-Juan, J. M.; Coronado, E.; Palií, A. V.; Tsukerblat, B. S. *Magnetic Properties of Mixed-Valence Systems: Theoretical Approaches and Applications*. In *Magnetoscience—From Molecules to Materials*; Miller, J., Drillon, M., Eds.; Wiley-VCH: Weinheim, 2001; p 155–210. (b) Borrás-Almenar, J. J.; Clemente-Juan, J. M.; Coronado, E.; Palií, A. V.; Tsukerblat, B. S. *J. Solid State Chem.* **2001**, *159*, 268–280.

(5) Yamase, T.; Fukaya, K.; Nojiri, H.; Ohshima, Y. *Inorg. Chem.* **2006**, *45*, 7698–7704.

(6) (a) Gatteschi, D.; Pardi, L. *Gazz. Chim. It.* **1993**, *123*, 231–240. (b) Bencini, A.; Gatteschi, D. *Electron Paramagnetic Resonance of Exchange Coupled Systems*; Springer: Berlin, 1990.

(7) (a) Borrás-Almenar, J. J.; Clemente-Juan, J. M.; Coronado, E.; Tsukerblat, B. S. *J. Comp. Chem.* **2001**, *22*, 985–991. (b) *Inorg. Chem.* **1999**, *38*, 6081–6088.

(8) Van Vleck, J. H. *The Theory of Electric and Magnetic Susceptibilities*; The Clarendon Press: Oxford, U.K., 1932.

(9) Earnshaw, A.; Figgis, B. N.; Lewis, J. J. *Chem. Soc. A* **1966**, 1656.

(10) Belorizky, E.; Fries, P. H. *J. Chim. Phys.* **1993**, *90*, 1077–1100.

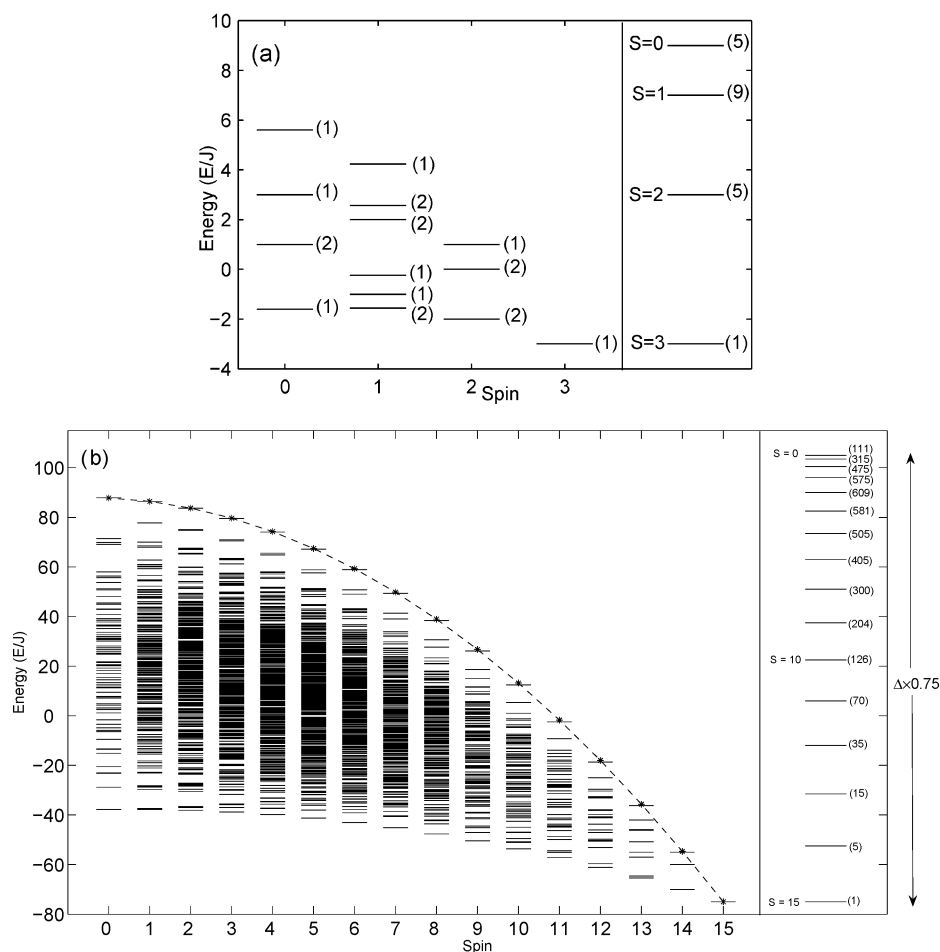


**Figure 2.** Energy levels for Cu<sub>6</sub> (a) and for Mn<sub>6</sub> (b) clusters in the first-neighbor coupling approximation. The additional multiplicities of spin states (number of the levels with the same  $S$ ) are indicated in parentheses. Left: Energy pattern calculated with MAGPACK. Right: Energy pattern calculated according to the Van Vleck formula. The energy pattern in the right side of b is scaled by 0.75. Dashed line represents the upper bound of the rotational band (see text). For the sake of clarity, the levels have been shifted by a constant to get the same ground state energies in both energy patterns.

cases the levels with a given  $S$  are independent of the sets of intermediate spins  $\{\tilde{S}\} = S_{12}S_{123}, S_{1234}, S_{12345}$  ( $S_{12} = S_1 + S_2$ , etc.) and are thus additionally degenerate according to the number  $n(S)$  of the possible sets  $\{\tilde{S}\}$  giving rise to a given full spin  $S$ . The labeling of the states does depend on the coupling scheme (that can be chosen in an alternative way), but the degeneracy of the  $S$  multiplets remains the same.

In a general case of a spin ring, in particular for a spin hexagon, the Kambe's formula is inappropriate even approximately, so that the matrix of the exchange Hamiltonian, eq 1, is to be diagonalized. This was understood long ago (for a review, see the book by Gatteschi et al.<sup>2</sup> and references therein), and during the past years, efficient theoretical approaches to the evaluation of the energy levels of spin rings have been developed.<sup>11</sup> In particular, six-membered

antiferromagnetic rings of different spins have been studied in detail<sup>11a,b,h</sup> within the exact and approximate approaches. To estimate the exchange parameters in Cu<sub>6</sub> and Mn<sub>6</sub>, we have calculated the energy pattern (eigenvalues of  $H_0 + H'$ ) by means of the MAGPACK software, a package to calculate the energy levels, bulk magnetic properties, and inelastic neutron scattering spectra of high nuclearity spin clusters,<sup>7</sup> based on the use of the ITO technique.<sup>2,6,12,13</sup> The energy levels for the Cu<sub>6</sub> and Mn<sub>6</sub> clusters as functions of the full-spin values are given in the left-hand parts of Figure 2a and b for the case of  $J = 0$ . The magnetic behavior investigated by magnetic susceptibility measurements was unambiguously shown<sup>5</sup> to be ferromagnetic, so that the energy patterns in Figure 2 correspond to  $J > 0$ . The energy levels derived from the Kambe's formula, eq 2, are represented in the right part of Figure 2a and b.

One can see that the levels within the "spherical" model obey Lande's rule and are substantially different from the

(11) (a) Waldmann, O. *Phys. Rev. B* **2002**, *65*, 024424/1–024424/13. (b) Waldmann, O. *Phys. Rev. B* **2000**, *61*, 6138–6144. (c) Schmidt, H.-J.; Schnack, J.; Luban, M. *Europhys. Lett.* **2001**, *55*, 105–111. (d) Schnack, J.; Luban, M.; Modler, R. *Europhys. Lett.* **2001**, *56*, 863–869. (e) Schnack, J.; Luban, M.; Modler, R. *Int. J. Mod. Phys. B* **2003**, *17*, 5053–5057. (f) Waldmann, O. *Europhys. Lett.* **2002**, *57*, 618–619. (g) Schmidt, H.-J.; Schnack, J.; Luban, M. *Europhys. Lett.* **2002**, *57*, 620–621. (h) Schnack, J. *Molecular Magnetism, Lecture Notes in Physics*; Springer-Verlag: Berlin, 2004; Vol. 645, p 155–194.

(12) (a) Tsukerblat, B. S.; Belinskii, M. I.; Fainzilberg, V. E. *Soviet Sci. Rev. B* **1987**, *9*, 337–481. (b) Tsukerblat, B. S., Belinskii, M. I. *Magnetochemistry and Radiospectroscopy of Exchange Clusters*; Pub. Stiintsa (Acad. Sci. Moldova): Kishinev, Moldova, 1983.

(13) Tsukerblat, B. S. *Group Theory in Chemistry and Spectroscopy*; Dover: Mineola, 2006.

exact energy pattern in the following, which has severe implications for the analysis of the magnetic data: (1) The full gap of the exchange splitting,  $\Delta = E(S_{\min}) - E(S_{\max})$ , in the “spherical” model exceeds the gap obtained in the exact calculation (12J vs 8.6J for Cu<sub>6</sub> and 240J vs 163J for Mn<sub>6</sub>; note that the energy pattern in the right side of Figure 2b is scaled by factor 0.75 for the sake of clarity). This feature becomes intuitively evident even from a qualitative consideration. In fact, the spherical Hamiltonian, eq 3 involves, along with first-neighbor interactions ( $H_0$ ), all possible (second- and third-neighbor) pairwise interactions ( $H'$ , etc.) with the same coupling parameter overestimating the full exchange energy. (2) The levels in the “spherical model” are highly degenerate according to the number  $n(S)$  of possible sets of the intermediate spin values (within a given coupling scheme) giving rise to a full spin  $S$ .

### 3. Symmetry Properties and Anisotropic Contributions

Point-symmetry assignment<sup>12,13</sup> of spin multiplets  $n(S)-D^{(S)}$  shows that they correspond to the sets of  $S\Gamma$  terms, corresponding the irreducible representations  $\Gamma$ (irreps) of  $C_{6v}$  point group (a general approach is given in ref 12). For example, using the approach described in ref 13, we get the following correlation for the Cu<sub>6</sub> ring:

$$\begin{aligned} D^{(3)} &\rightarrow {}^7B_2 \\ 5D^{(2)} &\rightarrow {}^5A_1 + {}^5E_1 + {}^5E_2 \\ 9D^{(1)} &\rightarrow {}^3A_2 + 2{}^3B_2 + {}^3E_2 + 2{}^3E_1 \\ 5D^{(0)} &\rightarrow 2{}^1A_1 + {}^1B_1 + {}^1E_1 \end{aligned} \quad (4)$$

One can see that the “accidentally” degenerate spin multiplets in the spherical model comprise orbitally degenerate states (irreps  $E_1$  and  $E_2$  in  $C_{6v}$ ) and orbital singlets  $A_1, A_2, B_1, B_2$ . For example, 9-fold degenerate  $S = 1$  levels in the spherical model involves three orbital singlets  ${}^3A_2, 2{}^3B_2$  and three orbital doublets  ${}^3E_2$  and  $2{}^3E_1$ . Only ferromagnetic ground state  $S = 3$  does not exhibit excessive degeneracy and is represented by the orbital singlet  ${}^7B_2$ . “Accidental” degeneracies (arising from a more general symmetry of the isotropic exchange Hamiltonian)<sup>12</sup> are removed in the calculated exact energy pattern (Figure 2). At the same time, the energy pattern exhibits exact doubly degenerate levels (irreps  $E_1$  and  $E_2$ ), for example, the first and second ( $S_{\max} - 1$ ) level for both Cu<sub>6</sub> and Mn<sub>6</sub>, etc. These degeneracies arise from the point symmetry of the system in the sense that they are associated with the definite terms  $S\Gamma$  of the systems and thus cannot be removed by the remaining isotropic interactions preserving hexagonal symmetry, for instance, by the next-neighbor interactions or biquadratic exchange. It also should be noted that the matrix of the HDVV Hamiltonian for Cu<sub>6</sub> cluster (including also all interactions) can be blocked on a symmetry-adapted basis and contains only two  $2 \times 2$  matrices corresponding  $2{}^3B_2$  and  $2{}^1A_1$  so that the eigenproblem in this case has an analytical solution (that is not given here). The dimensions of the  $S\Gamma$  blocks for Mn<sub>6</sub> are

much higher so that a numerical solution in this case is required. (3) The first excited level in the “spherical model” is much higher than that obtained in the exact calculation. Thus, for the Cu<sub>6</sub> and Mn<sub>6</sub> clusters the gaps  $\Delta_{2,3} = E(2) - E(3)$  and  $\Delta_{14,15} = E(14) - E(15)$  in the spherical model are 6J and 30J, respectively, while the exact values are J and 5J. Finally, an interesting similarity between the  $S_{\max} - 1$  sets of the levels is worth mentioning. One can see that the  $S = 2$  stack for Cu<sub>6</sub> consists of two doublets  $E_1, E_2$  and a singlet  $A_1$  separated by the gaps 2J and J (Figure 2a), and at the same time, the  $S = 14$  stack in Mn<sub>6</sub> contains  $E_1, E_2$ , and  $A_1$  with the same ratio of the gaps that are five times larger, 10J and 5J.

The group theoretical assignment allows one to elucidate the character of the anisotropy in the ground and excited states of the systems under consideration, which exhibit orbital degeneracy. The key issues can be illustrated by taking the simpler case of a Cu<sub>6</sub> hexagon as an example, for which the ground term is represented by the orbital singlet  ${}^7B_2$  and the set of the excited levels with  $S = 2$  involves two orbital doublets  ${}^5E_1$  and  ${}^5E_2$ . The ferromagnetic ground state for a spin ring is the only state (all spins “up”) and proves to be an orbital singlet (for example,  ${}^7B_2$  for Cu<sub>6</sub> hexagon). For the orbital singlet  ${}^7B_2$ , the orbital angular momentum contribution is reduced and only a second-order spin–orbital effect is present. The second-order spin–orbital interaction in this case leads to a uniaxial zero-field splitting that can be represented by the conventional Hamiltonian<sup>14–16</sup>

$$H_{\text{ax}} = D \left( S_Z^2 - \frac{1}{3} S(S+1) \right) \quad (5)$$

with  $Z$  along  $C_6$  axis, and only the bilinear contribution is taken into account.

Orbitally degenerate multiplets require inclusion of additional anisotropic interactions. To define them, let us note that the selection rules<sup>13</sup> for the matrix elements of the purely imaginary operator  $\mathbf{L}$  of the orbital angular momentum are defined by the decomposition of the antisymmetric parts  $\{E_1^2\}$  and  $\{E_2^2\}$  of the direct products  $E_1 \times E_1$  and  $E_2 \times E_2$ . In  $C_{6v}$  symmetry,  $\{E_1^2\} = \{E_2^2\} = A_2$ , so that only the  $L_Z$  component (irrep  $A_2$ ) of  $\mathbf{L}$  has non-vanishing matrix elements within the  $E_1$  and  $E_2$  basis sets. This means that the  ${}^5E_1$  and  ${}^5E_2$  terms are split by spin-orbital interaction and only the  $\lambda L_Z S_Z$  part of spin-orbital coupling  $H_{\text{SO}}$  is active. In the spin-coupling scheme, the AS exchange interaction introduced by Dzyaloshinsky and Moria<sup>17</sup> (where  $\mathbf{D}_{ij}$  are the vector parameters), eq 6

$$H_{\text{AS}} = \sum_{ij} \mathbf{D}_{ij} [\mathbf{S}_i \times \mathbf{S}_j] \quad (6)$$

(14) Kahn, O. *Molecular Magnetism*; VCH: New York, 1993.

(15) Böca, R. *Theoretical Foundations of Molecular Magnetism*; Elsevier: Amsterdam, 1999.

(16) (a) Böca, R. *Coord. Chem. Rev.* **1998**, *173*, 167–283. (b) Böca, R. *Coord. Chem. Rev.* **2004**, *248*, 757–815.

(17) (a) Dzyaloshinskii, I. E. *Zh. Exp. Teor. Fiz.* **1957**, *32*, 1547 [*Sov. Phys. JETP* **1957**, *5*, 1259]. (b) Moria, T. *Phys. Rev.* **1960**, *120*, 91.

is equivalent to spin-orbital interaction in  $5E_1$  terms,<sup>12,13</sup> and thus we arrive at the conclusion that the AS exchange appears and only the z-component (normal part) of the AS exchange

$$H_{AS}^{\parallel} = \sum_{ij} D_{ij}^Z [S_i \times S_j]_z \quad (7)$$

operates within the  $^5E_1$  and  $^5E_2$  bases and splits these multiplets. When orbital degeneracy is present, the AS exchange acts as a first-order effect with respect to the spin-orbital interaction and for this reason, in general, exceeds the zero-field term, eq 5, that appears as a second-order effect<sup>15,16</sup> and gives also nonzero contribution for all terms with  $S \geq 1$ , along with the AS exchange. It should be underlined that in the case of orbitally degenerate multiplets the conventional zero-field term, eq 5, plays a secondary role. Because of the above-mentioned similarity of the  $S = 2$  stack for  $Cu_6$  and the  $S = 14$  stack in  $Mn_6$  the same conclusion is valid for  $^{29}E_1$  and  $^{29}E_2$  multiplets of  $Mn_6$ . From the viewpoint of symmetry, the role of the “in-plane” component of the AS exchange, eq 8

$$H_{AS}^{\perp} = \sum_{ij} (D_{ij}^X [S_i \times S_j]_X + D_{ij}^Y [S_i \times S_j]_Y) \quad (8)$$

can be understood by considering of the selection rules for the off-diagonal matrix elements of the  $L_X$  and  $L_Y$  components (irrep  $E$ ) of  $\mathbf{L}$  that are defined by the decomposition of the direct products (but not antisymmetric parts as in the case so far discussed),  $\Gamma_1 \times \Gamma_2$ , where  $\Gamma_1$  and  $\Gamma_2$  are the irreps corresponding to the orbital part of the exchange multiplets. Additionally, spin-orbital mixing occurs, providing  $\Delta S = 0, 1$  (selection rule for the first rank spin tensor). For example, in the  $Cu_6$  ring, the ground term  $^7B_2$  is mixed by the in-plane part of AS exchange only with the  $^5E_2$  term from the  $S = 2$  stack (in fact,  $B_2 \times E_2 = E_1(L_X, L_Y)$ ), while the mixing of  $^7B_2$  with the second orbital doublet  $^5E_1$  is forbidden (the direct product  $B_2 \times E_1 = E_2$ , that is, does not contain  $E_1(L_X, L_Y)$ ). Since normally the isotropic exchange is the leading interaction, the mixing acts as a second-order perturbation within each  $5E_1$  multiplet and, in particular, contributes to the zero-field splitting of the ground state  $^7B_2$ . At the same time, the AS mixing modifies the AS exchange splitting in the excited term  $^5E_2$ . The remaining multiplets can be considered in the same way. Quite a similar observation of the different role of the normal and in-plane components' AS exchange has been made for the case of the triangular vanadium moiety in  $V_{15}$  molecule.<sup>18</sup> Symmetry considerations show that this result seems to be common for the spin rings with actual axial symmetry for which a  $C_n$  axis ( $n \geq 3$ ) is present.

Recently, a very large AS exchange was evoked by Solomon with co-workers<sup>19</sup> in his study of the unusual properties of tri-copper clusters. In view of the results of ref 19, one can expect significant AS exchange in the excited

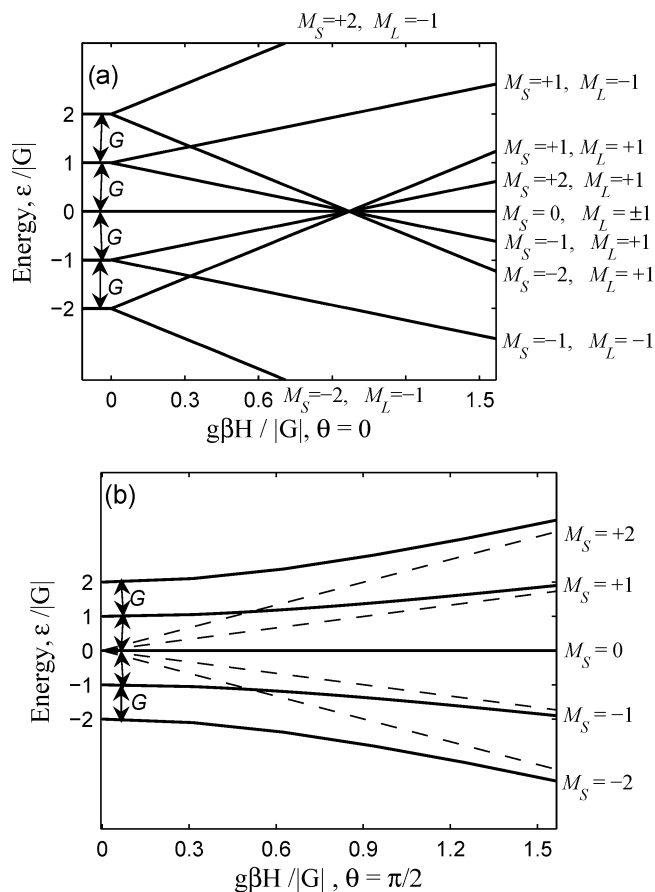


**Figure 3.** Zero-field splitting of  $^5E_1$  term by the AS exchange and Zeeman splitting in the magnetic field applied along  $C_6$  axis (a) and in the plane of the hexagon (b).

states of  $Cu_6$  rings and significant second-order effects that should contribute to the magnetization. Very strong isotropic exchange has recently been found in copper(II) hexanuclear rings, in which one can also expect strong AS exchange.<sup>20</sup> The second-order effects (zero-field splitting) in the triangular  $Cu_3$  systems have recently been considered by Belinsky.<sup>21</sup>

Finally, let us illustrate the anisotropic properties of the AS exchange by consideration of the excited exchange multiplets exhibiting orbital degeneracy, for which a first-order splitting is caused by  $H_{AS}^{\parallel}$ . Figure 3 shows the calculated splitting of the excited degenerate level  $^5E_1$  of the  $Cu_6$  cluster by the normal part of the AS exchange and the Zeeman splitting in two principal directions of the applied magnetic field, along the  $C_6$  axis and in the plane of the hexagon. One can see that the normal part of AS exchange splits  $^5E_1$  into five equally spaced doublets. Since the basis  $E_1$  can be associated with the two functions with the projection  $M_L = \pm 1$  of the orbital angular momentum the basis of the doublets can be labeled as  $|S M_S M_L\rangle \equiv |M_S M_L\rangle$ :  $|M_S M_L\rangle = |\pm 2, \pm 1\rangle, |\pm 1, \pm 1\rangle, |0, \pm 1\rangle, |\pm 1, \mp 1\rangle, |\pm 2, \mp 1\rangle$ .

(18) (a) Tsukerblat, B.; Tarantul, A.; Müller, A. *Phys. Lett. A* **2006**, *353*, 48. (b) Tarantul, A.; Tsukerblat, B.; Müller, A. *Inorg. Chem.* **2007**, *46*, 161–169.  
 (19) Yoon, J.; Mirica, L. M.; Stack, T. D. P.; Solomon, E. I. *J. Am. Chem. Soc.* **2004**, *126*, 12586–12595.

(20) Mohamed, A. A.; Burini, A.; Galassi, R.; Paglialunga, D.; J. R. Galán-Mascarós, J. R.; Dunbar, K. R.; Fackler, J. P., Jr. *Inorg. Chem.* **2007**, *46*, 2348–2349.  
 (21) Belinsky, M. The optimization of the composition, structure and properties of metals, oxides, composites, nano- and amorphous materials. *Proceedings of the Sixth Israeli–Russian Workshop*; Israeli Academy of Sciences: Jerusalem, 2007; pp. 98–116.

The doublets can be labeled by the values of the  $|M_J\rangle$  where  $M_J = M_S + M_L$  is the quantum number of the total angular momentum projection that is a good quantum number in the case of axial symmetry. The eigen-functions in the  $M_J$ -basis are  $|M_J\rangle = |\pm 3\rangle, |\pm 2\rangle, |\pm 1\rangle, |0\rangle$  (twice),  $|\pm 1\rangle$ . With the use of the Magpack software, these basis functions are expressed in terms of the initial spin basis  $|S_{12} S_{123} S_{1234} S_{12345} S M\rangle$ . For the  ${}^5E_1$  term, the  $H_{AS}^{\parallel}$  term leads to five equidistant doublets with energies  $\epsilon(M_S M_L) = GM_L M_S$ . The straightforward diagonalization of  $H_{AS}^{\parallel}$  gives the gaps  $G = D_n/\sqrt{3}$  and  $D_n/\sqrt{15}$  for two doublets in the  $S = 2$  stack of  $\text{Cu}_6$  as shown in Figure 3a for  ${}^5E_1$ . For the sake of simplicity, the Zeeman interaction is assumed to be isotropic, and only the leading spin part is taken into account. Figure 3a shows the linear Zeeman splitting of the doublets  $G M_L M_S \pm g\beta M_S H$  in parallel ( $H\parallel C_6$ ) field, the  $g$ -factors of the system coinciding with  $g$ -factors of the constituent ions. It is remarkable that the Zeeman sublevels cross at  $H_{\text{cross}} = |G|/g\beta$ . For any in-plane direction, the field the energies at low fields are quadratic in the field (second-order effect), while in the limit of the strong field, one finds five double degenerate sublevels,  $g\beta M_S H$ , that are independent of  $G$  and simply coincide with those for spin  $S$  in absence of anisotropic interactions. This can be understood as the effect of reduction of the AS exchange by a strong field along the hard axis of magnetization (in-plane direction). The levels in this limit simply represent the Zeeman pattern corresponding to the new quantization axis lying in the plane. Consequently, the  $M_S$  labels in Figure 3b are related to the dashed levels and correspond to the in-plane axis of spin quantization (rather than to the  $C_6$  axis as in Figure 3a). A more detailed study of the consequences of the AS exchange in EPR pattern will be given elsewhere.

#### 4. Magnetic Susceptibility and Magnetization

The molar magnetization and magnetic susceptibility are subsequently obtained with the use of the conventional expressions<sup>15,16</sup>

$$M_{\alpha}(H, T) = NkT \frac{\partial \ln Z}{\partial H_{\alpha}} \quad \chi_{ab} = NkT \frac{\partial^2 \ln Z}{\partial H_{\alpha} \partial H_{\beta}} \quad (9)$$

The saturation values of the magnetization ( $M_{\text{sat}} = gS$ ) as functions of applied field, assuming ferromagnetic ground states  $S = 3$  and 15 for  $\text{Cu}_6$  and  $\text{Mn}_6$  clusters, allows us to estimate effective  $g$ -factors that are 2.2 and 1.93 for  $\text{Cu}_6$  and  $\text{Mn}_6$ , respectively (see below). In the fitting of the experimental data<sup>5</sup> on magnetization versus field (at 1.8K), we employ the so-called ‘‘giant-spin approximation’’,<sup>2,6</sup> assuming that the ground states ( $S = 3$  and 15) are well enough isolated and neglecting the mixing of these states with the excited ones through the anisotropic contributions. In fact, the gaps  $\Delta_{2,3}$  and  $\Delta_{14,15}$  estimated with the best-fit parameters,  $J$ , are 35 ( $\text{Cu}_6$ ) and 2.75  $\text{cm}^{-1}$  ( $\text{Mn}_6$ ) (see below), which indicates that the excited levels are weakly populated even in the low-field region. It is also noteworthy that as the applied field increases, the levels become even more pronouncedly isolated. As was demonstrated in the book by Gatteschi

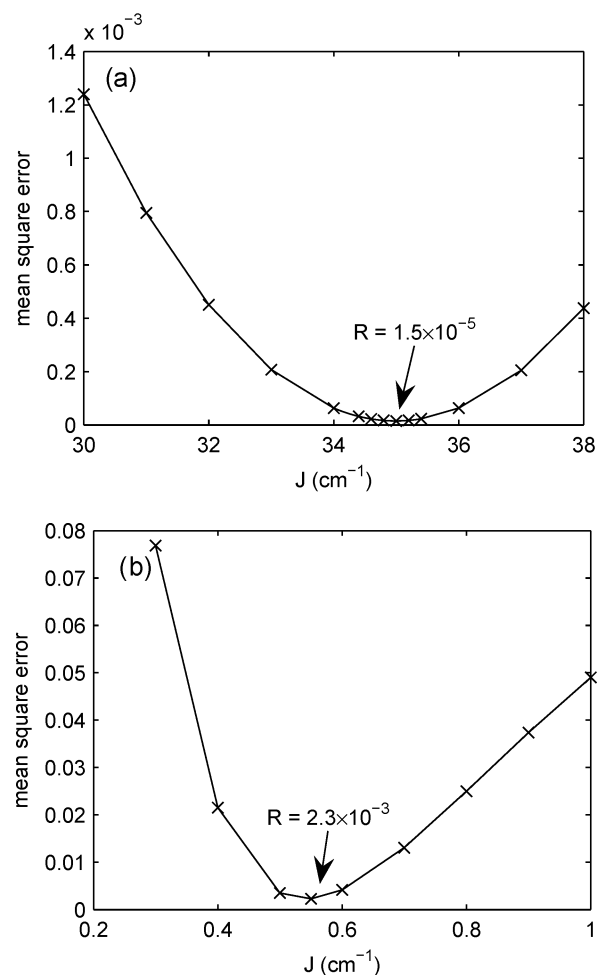


**Figure 4.** Mean-square error as a function of the parameter  $J$  for  $\text{Cu}_6$  (a) and  $\text{Mn}_6$  (b) clusters.

et al.,<sup>2</sup> the analysis of magnetization in a powder with a simple conventionally accepted averaging formula,  $M = (1/3)M_{\parallel} + (2/3)M_{\perp}$ , can give an error in the dependence  $M(H, T)$ . In view of this observation, we have made a least-square analysis of the calculated magnetic susceptibility  $M$  with the use of the exact averaging based on integration over two polar angles and also in a simple model. The mean square error factor  $R$  is defined as usual,  $R = \sum (M_{\text{exp}} - M_{\text{calcd}})^2 / N M_{\text{exp}}^2$ , where  $N$  is the number of the experimental points. In the case under consideration, the  $D$  values obtained in simple and exact models of powder averaging provide close results. The calculated average magnetization versus field, for  $\text{Cu}_6$  (Figure 5a) shows good fit to the Brillouin function with  $g = 2.2$  ( $R = 9.8 \times 10^{-4}$ ), whereas for  $\text{Mn}_6$ , the fit to the Brillouin function (Figure 5b) is poor at intermediate fields ( $R = 0.026$ ). Deviation of the magnetization at intermediate fields, which can be attributed to magnetic anisotropy, has been taken into account in the framework of the conventional uniaxial zero-field splitting Hamiltonian,<sup>13–16</sup> eq 5, that is valid for spin multiplets in the absence of the orbital degeneracy. This has largely improved the fit, reducing  $R$  to  $1.6 \times 10^{-4}$  for  $\text{Cu}_6$  and  $9.0 \times 10^{-4}$  for  $\text{Mn}_6$ , the influence of the anisotropy being especially pronounced for  $\text{Mn}_6$ . As one can see from Figure 5b, the inclusion of the anisotropic term dramatically changes the shape of magnetization versus

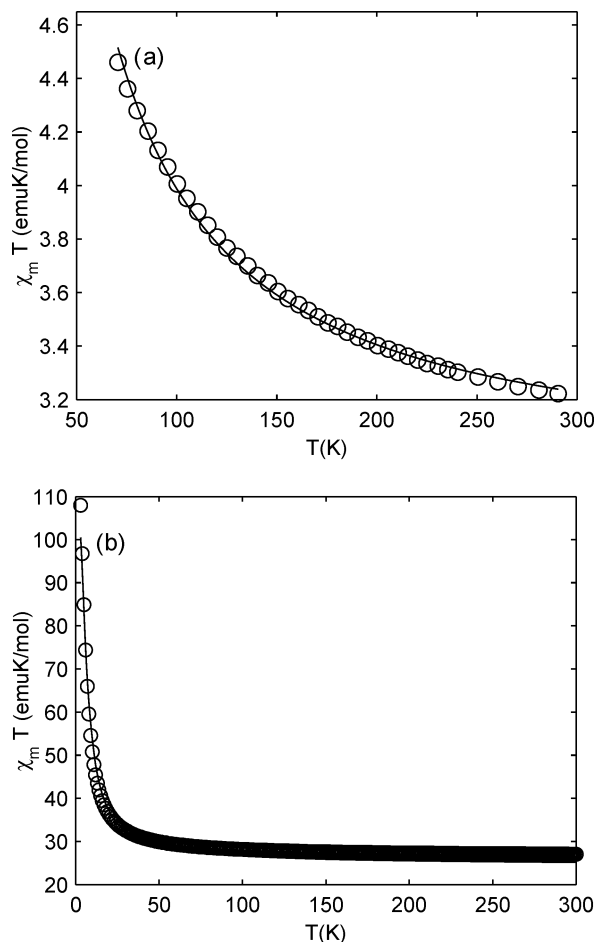


**Figure 5.** Temperature dependence of the magnetic susceptibility for Cu<sub>6</sub> (a) and Mn<sub>6</sub> (b) clusters. Circles represent the experimental values derived from ref 5, and the solid lines represent the calculated values for the best-fit parameters, see text.

field curve for Mn<sub>6</sub> and perfectly explains the occurrence of a broad peculiar shoulder at intermediate fields. For Cu<sub>6</sub>, the zero-field splitting parameter  $D$ , which yields the best fit, is negative,  $D = -0.23 \text{ cm}^{-1}$ , and differs somewhat from that ( $D = -0.127 \text{ cm}^{-1}$ ) deduced from the analysis of the EPR experiments,<sup>5</sup> while for Mn<sub>6</sub>, we found a positive  $D$  that is  $0.09 \text{ cm}^{-1}$ . It was noted in ref 5 that the observed fine structure of the EPR pattern of Cu<sub>6</sub> is not equidistant, and the authors explained this observation by possible importance of the next order contributions in the zero-field splitting. This can explain also the difference between the so far obtained value of  $D$  by fitting of magnetization and that found from EPR in ref 5. High-order terms contain new adjustable parameters that would result in the excessive flexibility of the theoretical model. More detailed EPR data (for example, angular dependence) in conjunction with a more full theoretical model are expected to precisely generate the  $D$  parameter in the Cu<sub>6</sub> system. The effective values  $DS^2$  of the anisotropy parameters in Mn<sub>6</sub> are not small enough to fully justify the use of the giant spin model, so that, for a full description of Mn<sub>6</sub>, one should go beyond limitations of this model.

To reduce the number of the adjustable parameters, we will use the values of the  $g$ -factors obtained in the fit of

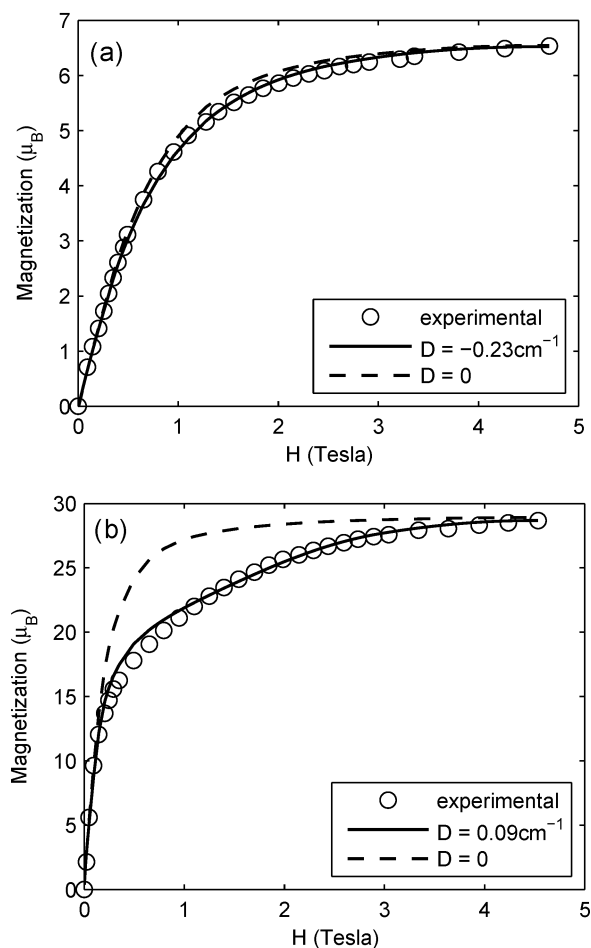


**Figure 6.** Field dependence of magnetization ( $T = 1.8 \text{ K}$ ) for Cu<sub>6</sub> (a) and Mn<sub>6</sub> (b) clusters. Circles represent the experimental values derived from ref 5, and the solid lines represent the calculated values for the best fit parameters (see text); the dotted lines represent the Brillouin function.

magnetization to fit the data on magnetic susceptibility. Experimental data on the molar magnetic susceptibility ( $\chi_m$  and  $\chi_m T$ ) for polycrystalline samples at low magnetic fields (0.1 and 0.05 T for Cu<sub>6</sub> and Mn<sub>6</sub>, respectively) are reported in ref 5. A least-square analysis of the calculated magnetic susceptibility  $\chi$  with a simple averaging formula  $\chi = (1/3)\chi_{\parallel} + (2/3)\chi_{\perp}$  yields the best fit to the experimental results thus, providing values for the exchange parameters. We found that, for Cu<sub>6</sub>,  $J = 35 \text{ cm}^{-1}$  and  $J' = 0$  with an error factor of  $R = 1.5 \times 10^{-5}$  and, for Mn<sub>6</sub>,  $J = 0.55 \text{ cm}^{-1}$  and  $J' = 0.01 \text{ cm}^{-1}$  with  $R = 2.3 \times 10^{-3}$ . Figure 3 shows that the error factor  $R$  as a function of the parameter  $J$  has a deep minimum, while the numerical analysis shows that the results are less stable with respect to  $J'$ . One can conclude that the stability of the fit is low; the fit does not allow one to accurately estimate  $J'$ , but the analysis shows that this parameter is definitely small. The temperature dependence of the magnetic susceptibility shows a very good fit of the calculated curves to the experimental results as shown in Figure 4. Since the parameter  $J'$  is negligible for Cu<sub>6</sub> and very small for Mn<sub>6</sub>, one can compare the values of  $J$  obtained in our fit with those reported in ref 5, namely,  $8.82 \text{ cm}^{-1}$  for Cu<sub>6</sub> and  $0.14 \text{ cm}^{-1}$  for Mn<sub>6</sub>. One can see that the theoretical model for a spin hexagon based on the Kambe–

Van Vleck equation results in an essential underestimation of  $J$ . This follows from an overestimation of the gaps in the energy pattern in this model, in particular, the gap between the ground and first excited level (Figure 2).

One can see that the HDVV model supplemented by the relatively small anisotropic terms provides a good description of the spin hexagons  $\text{Cu}_6$  and  $\text{Mn}_6$  in complex POMs, while application of a simple expression for spin levels  $-JS(S+1)$  gives incorrect estimation for the exchange parameters. It was recently demonstrated (Schmidt et al.<sup>11c</sup> and Schnack et al.)<sup>11d,e</sup> that in many HDVV systems (as discussed by Waldmann<sup>11f</sup> and Schmidt et al.)<sup>11g</sup> the energy pattern is approximately bounded by two parabolic curves (the upper bound for  $\text{Mn}_6$  is shown in Figure 2) so that the low lying levels involving all spin values form so-called rotational band,  $E(S) = -J_{\text{eff}}S(S+1)$ . Under some assumptions, the interrelation between the real and effective parameters can be found (see refs 11 and 2). The case of a ring with the first-neighbor coupling is favorable for the rotational band approximation<sup>11</sup> (especially for high spin ions), although in the case of a ferromagnetic ring the limitations are more severe. Nevertheless for the  $\text{Mn}_6$  ring of  $(n\text{-BuNH}_3)_{12}\text{[(MnCl)}_6(\text{SbW}_9\text{O}_{33})_2]\cdot 6\text{H}_2\text{O}$  with a relatively weak ferromagnetic exchange the two low-lying levels with  $S = 12$  and the excited level  $S = 14$  are very close in energy, and the remaining levels are not well isolated from the lower rotational band (Figure 2). These levels are well populated at  $T > 5$  K so that for a reliable description of the experimental data in the case under consideration the whole set of the levels is to be taken into account.

Finally, although the spin dependences of the energy levels in the rotational band approximation and in the spherical model are the same, giving rise to a Lande' rule of intervals, the multiplicities of degeneracy of the levels are different. The former takes into account only a part of the full spectrum

(possessing a specific set of degenerate levels) and uses an effective  $J$  parameter (that is different from the first-neighbor one), while the spherical model deals with a true exchange and results in the high accidental degeneracy as discussed. For these reasons, application of spherical model cannot be justified in terms of the rotational band approximation.

#### 4. Summary

In this paper, we have examined the spin levels and magnetic properties of two POMs, two novel polyoxotungstates,  $(n\text{-BuNH}_3)_{12}[(\text{CuCl})_6(\text{AsW}_9\text{O}_{33})_2]\cdot 6\text{H}_2\text{O}$  and  $(n\text{-BuNH}_3)_{12}[(\text{MnCl})_6(\text{SbW}_9\text{O}_{33})_2]\cdot 6\text{H}_2\text{O}$ , containing  $\text{Cu}_6^{12+}$  and  $\text{Mn}_6^{12+}$  hexagons. We have demonstrated the inapplicability of the Kambe–Van Vleck formula to a spin hexagon and successfully reproduced the experimental results on magnetic susceptibility and magnetization on the basis of the exact diagonalization of the HDVV Hamiltonian. The best fitting parameters exceed substantially those obtained within the “spherical model”. The results imply the importance of the uniaxial anisotropy which is shown to be especially pronounced for the  $\text{Mn}_6^{12+}$  cluster. We also discuss the group theoretical assignment of the exchange multiplets, their degeneracies, and symmetry rules for the AS exchange in the ground and excited states of the spin-rings. We also show how the symmetry rules are related to the anisotropic interactions and, in this view, analyze the manifestations of the AS exchange in orbitally degenerate multiplets. We underline also different roles of the normal and in-plane components of the AS exchange in the spin ring with an axial symmetry.

**Acknowledgment.** N.Z. thanks the Kreitman Foundation Fellowship for support. We thank the referees for *Inorganic Chemistry* for their helpful comments.

IC700585C